

Ferrocenylpyrazolyl bridging rhodium dimers. Crystal structure of $[\text{Rh}(\mu\text{-pz}^{\text{Fc}})(\text{COD})]_2$

José A. Campo ^{a,*}, Mercedes Cano ^{a,1}, José V. Heras ^a, Elena Pinilla ^{a,b},
Marta Ruiz-Bermejo ^a, Rosario Torres ^b

^a Departamento de Química Inorgánica I, Facultad de Ciencias Químicas, Universidad Complutense, E-28040 Madrid, Spain

^b CAI de Difracción de Rayos-X, Facultad de Ciencias Químicas, Universidad Complutense, E-28040 Madrid, Spain

Received 23 November 1998

Abstract

The ability of pyrazolato ligands to form dinuclear complexes has been used to prepare a family of rhodium(I) complexes of the type $[\text{Rh}(\mu\text{-pz}^{\text{Fc}})(\text{L}_2)]_2$ ($\text{L}_2 = 2,5\text{-norbornadiene (NBD) (1)}$; $1,5\text{-cyclooctadiene (COD) (2)}$; 2CO (3)) containing ferrocenylpyrazolate (pz^{Fc}) as a bridging ligand. The diolefinic compounds **1** and **2** were obtained as the head-to-tail (H-T) isomer, whereas the tetracarbonyl derivative **3** was formed as a mixture of the head-to-tail (H-T) and head-to-head (H-H) isomers, as deduced by NMR studies in solution. The crystal structure determination of $[\text{Rh}(\mu\text{-pz}^{\text{Fc}})(\text{COD})]_2$ confirmed its identity as the H-T isomer having the boat conformation for the six-membered $\text{Rh}(\text{NN})_2\text{Rh}$ ring in the solid state. Important structural parameters were $\text{Rh}\cdots\text{Rh}$ and $\text{Rh}\cdots\text{H10}$ distances of 3.189(1) and 2.877 Å, respectively, according to the presence of weak intermolecular interactions. Electronic and electrochemical studies were also performed. © 1999 Elsevier Science S.A. All rights reserved.

Keywords: Ferrocenylpyrazole; Rhodium–pyrazolate dimers; X-ray structure; Conformational isomerism

1. Introduction

The design of systems which undergo electron-transfer processes [1] is very interesting as models for molecular electronics [2]. Some of these systems with applications in nonlinear optical materials [3], electronic devices [4] and catalysis [5] have been shown to have the ferrocenyl group as a redox-active center due to its characteristic redox behavior.

The use of pyrazol groups covalently linked to ferrocenyl moieties as bridging ligands to produce poly-metallic species is very promising from the point of view of possible intramolecular electron-transfer processes for catalytic purposes [6]. The incorporation of ferrocenyl substituents in pyrazol groups was reported in the early 1960s [7]. However, despite the versatility of pyrazoles as ligands or bridging blocks in polydentate

ligands for metal ions [8], ferrocenylpyrazoles have not been widely studied [9–14].

On the other hand it is noticeable that there is a great number of reports dealing with bridged dimeric rhodium(I) complexes containing substituted pyrazolato ligands [15–20]. The majority of these complexes have been found to have two pyrazolato ligands bridging two rhodium atoms giving rise to a six-membered boat-shaped $\text{Rh}(\text{NN})_2\text{Rh}$ metallocyclic core. Most of these complexes have been shown to be non-rigid in solution by variable temperature NMR studies and the fluxional behavior generally associated with the boat–boat inversion of the six-membered $\text{Rh}(\text{NN})_2\text{Rh}$ metallocycle [18,20,21]. A complete thermodynamic study of this behavior has recently been carried out by Oro et al. [18].

However, in a previous work [19] we found a static conformation of the $\text{Rh}(\text{NN})_2\text{Rh}$ boat in the complexes $[\text{Rh}(\mu\text{-pz}^{\text{R}})(\text{L}_2)]_2$ ($\text{R} = \text{C}_6\text{H}_4\text{OC}_6\text{H}_5$, $\text{C}_6\text{H}_4\text{OC}_4\text{H}_9$; $\text{L}_2 = 2,5\text{-norbornadiene (NBD)}$, $1,5\text{-cyclooctadiene (COD)}$, 2CO), this behavior being considered a consequence of weak intramolecular interactions between the rhodium atom and the substituents on the pyrazole groups.

* Corresponding author. Fax: +34-91-3944352.

E-mail addresses: jacampo@eucmax.sim.ucm.es (J. Campo), mmcano@eucmax.sim.ucm.es (M. Cano)

¹ Also corresponding author.

Following these precedents we report here the synthesis and properties of binuclear rhodium(I) complexes $[\text{Rh}(\mu\text{-pz}^{\text{Fc}})(\text{L}_2)]_2$ ($\text{L}_2 = \text{NBD}$ (**1**), COD (**2**), 2CO (**3**)) containing ferrocenylpyrazolate (pz^{Fc}) as a bridging ligand. The study focused on the analysis of potential interactions between the ferrocenyl groups and the rhodium atom and the electronic effects produced by the redox active sites.

2. Experimental

2.1. Materials

All commercial reagents were used as supplied. The reactions were performed at room temperature (r.t.) under dry oxygen-free dinitrogen. Commercial solvents were degassed prior to use. The starting Rh-complexes $[\text{Rh}(\mu\text{-Cl})(\text{L}_2)]_2$ ($\text{L}_2 = \text{NBD}$, COD) and the 3(5)-(ferrocen-1-yl)pyrazole ligand were synthesized by literature procedures [9,22].

2.2. Physical measurements

Elemental analyses for carbon, hydrogen and nitrogen were carried out by the Microanalytical Service of the Complutense University. IR spectra were recorded on an FT-IR Nicolet Magna-550 spectrophotometer with samples as KBr discs in the $4000\text{--}350\text{ cm}^{-1}$ region or in a dichloromethane solution in the $2500\text{--}1800\text{ cm}^{-1}$ region. FAB mass spectra were obtained on a VG AutoSpec spectrometer.

^1H - and $^{13}\text{C}\{^1\text{H}\}$ -NMR spectra were performed on a Varian VXR-300 (299.95 and 75.40 MHz for ^1H - and ^{13}C -, respectively) and on a Bruker AM-300 (300.13 and 75.43 MHz for ^1H - and ^{13}C -, respectively) spectrophotometer of the NMR Service from solutions in CDCl_3 . Chemical shifts δ are listed in ppm relative to TMS using the signal of the deuterated solvent as reference; coupling constants J are in Hz. The ^1H - and ^{13}C - chemical shifts are accurate to 0.01 and 0.1 ppm, respectively. Coupling constants are accurate to ± 0.3 Hz for ^1H -NMR spectra and ± 0.6 Hz for ^{13}C -NMR spectra. The homonuclear (^1H - ^1H)COSY spectra were recorded on the latter spectrometer.

The electronic spectra were registered on a CARY 5G spectrophotometer with solutions of ca. 10^{-4} M of the complexes in dichloromethane.

Cyclic voltammetric measurements were carried out on an Autolab apparatus equipped with a PSTA 10 potentiostat using a three-electrode cell with platinum wire as working and auxiliary electrodes and an $\text{Ag}|\text{AgCl}$ electrode as a reference, with a solution (ca. 10^{-3} mol dm^{-3}) of the complex in dichloromethane containing $[\text{NBu}_4][\text{BF}_4]$ (0.2 mol dm^{-3}) as the base electrolyte, using a scan rate of 200 mV s^{-1} . Values

are referred to an $\text{Ag}|\text{AgCl}$ electrode, but ferrocene was used as the internal standard.

2.3. Synthetic methods

2.3.1. Preparation of $[\text{Rh}(\mu\text{-pz}^{\text{Fc}})(\text{NBD})]_2$ (**1**)

2.3.1.1. Method A. To a suspension of $[\text{Rh}(\mu\text{-Cl})(\text{NBD})]_2$ (93 mg, 0.2 mmol) in methanol (15 ml) was added 3-ferrocenylpyrazole (100 mg, 0.4 mmol). To the clear orange solution immediately formed was added a solution of KOH in methanol (5 ml) in aliquots of 1 ml during a period of 30 s, and an orange solid precipitated. The mixture was stirred for 30 min and the solid was filtered off, washed with cold methanol and hexane and dried in vacuo (140 mg, 78%).

2.3.1.2. Method B. To a solution of $[\text{Rh}(\mu\text{-Cl})(\text{NBD})]_2$ (93 mg, 0.2 mmol) in dichloromethane (15 ml) was added triethylamine (361 mg, 0.5 ml, 3.57 mmol) followed by 3-ferrocenylpyrazole (100 mg, 0.4 mmol). After 2 h of stirring water (15 ml) was added and the organic layer separated off. The organic fraction was dried over sodium sulphate and then filtered. From the clear solution the desired product was precipitated with methanol, filtered off, washed with cold methanol and dried in vacuo (125 mg, 70%).

$[\text{Rh}(\mu\text{-pz}^{\text{Fc}})(\text{NBD})]_2$. Anal. Calc. for $\text{C}_{40}\text{H}_{38}\text{Fe}_2\text{N}_4\text{Rh}_2$: C, 53.84; H, 4.30; N, 6.28%. Found: C, 53.38; H, 4.03; N, 6.00%. IR (KBr, cm^{-1}): 1588 $\nu(\text{CN})$; 1105 $\nu(\text{CC})$; 812 $\pi(\text{CH})$; 1302 $\beta(\text{NBD})$. MS (FAB⁺, m/z): 892 $[\text{M}]^+$, 827 $[\text{M}-\text{C}_5\text{H}_5]^+$, 708 $[\text{M}-2\text{NBD}]^+$, 641 $[\text{M}-\text{pz}^{\text{Fc}}]^+$, 446 $[\text{M}/2]^+$.

2.3.2. Preparation of $[\text{Rh}(\mu\text{-pz}^{\text{Fc}})(\text{COD})]_2$ (**2**)

2.3.2.1. Method A. To a suspension of $[\text{Rh}(\mu\text{-Cl})(\text{COD})]_2$ (99 mg, 0.2 mmol) in methanol (15 ml) was added a solution of KOH in methanol (1 ml) followed by 3-ferrocenylpyrazole (100 mg, 0.4 mmol). (Note: it is important to carry out the addition of reactants in the indicated order to avoid the precipitation of the complex $[\text{Rh}(\text{Cl})(\text{Hpz}^{\text{Fc}})(\text{COD})]$ [23].) After a few minutes stirring an orange–yellow solid precipitated, and the mixture was stirred for a further 30 min. The solid was filtered off, washed with cold methanol and hexane and dried in vacuo (166 mg, 90%).

2.3.2.2. Method B. To a solution of $[\text{Rh}(\mu\text{-Cl})(\text{COD})]_2$ (99 mg, 0.2 mmol) in dichloromethane (15 ml) was added triethylamine (361 mg, 0.5 ml, 3.57 mmol) followed by 3-ferrocenylpyrazole (100 mg, 0.4 mmol). An orange–yellow precipitate immediately formed. After

30 min stirring, the solid was filtered off, washed with cold methanol and dried in vacuo (137 mg, 74%).

$[\text{Rh}(\mu\text{-pz}^{\text{Fc}})(\text{COD})]_2$. Anal. Calc. for $\text{C}_{42}\text{H}_{46}\text{Fe}_2\text{N}_4\text{Rh}_2$: C, 54.57; H, 5.03; N, 6.06%. Found: C, 54.19; H, 4.80; N, 6.01%. IR (KBr, cm^{-1}): 1589 $\nu(\text{CN})$; 1106 $\nu(\text{CC})$; 815 $\pi(\text{CH})$; 1274 $\beta(\text{NBD})$. MS (FAB⁺, m/z): 924 $[\text{M}]^+$, 859 $[\text{M}-\text{C}_5\text{H}_5]^+$, 708 $[\text{M}-2\text{COD}]^+$, 673 $[\text{M}-\text{pz}^{\text{Fc}}]^+$, 563 $[\text{M}-\text{pz}^{\text{Fc}}-\text{COD}]^+$, 462 $[\text{M}/2]^+$.

2.3.3. Preparation of $[\text{Rh}(\mu\text{-pz}^{\text{Fc}})(\text{CO})]_2$ (3)

Carbon monoxide was bubbled about ca. 30 min through a solution of **1** or a suspension of **2** (0.2 mmol) in dichloromethane (20 ml) at r.t. and atmospheric pressure. The initial yellow–orange colour of the solution changed to deep orange. By removing the solvent an orange–red oil was obtained which was treated with cold diethyl ether and evaporated again to dryness giving rise to a yellow–orange solid. This product was washed with cold hexane and dried in vacuo. Yield was practically quantitative.

$[\text{Rh}(\mu\text{-pz}^{\text{Fc}})(\text{CO})_2]_2$ (3). Anal. Calc. for $\text{C}_{30}\text{H}_{22}\text{Fe}_2\text{N}_4\text{O}_2\text{Rh}_2$: C, 43.94; H, 2.71; N, 6.83%. Found: C, 44.20; H, 2.83; N, 6.70%. IR (KBr, cm^{-1}): 2086, 2072, 2016 $\nu(\text{CO})$; 1588 $\nu(\text{CN})$; 1105 $\nu(\text{CC})$; 812 $\pi(\text{CH})$. MS (FAB⁺, m/z): 819 $[\text{M}]^+$, 792 $[\text{M}-\text{CO}]^+$, 763 $[\text{M}-2\text{CO}]^+$, 735 $[\text{M}-3\text{CO}]^+$, 706 $[\text{M}-4\text{CO}]^+$.

2.4. X-ray structure determination

Yellow prismatic single crystals of **2** were obtained from dichloromethane–acetonitrile. The data were collected on an Enraf–Nonius CAD4 diffractometer, and unit cell constants were refined from least squares fitting of the θ values of 25 reflections with 2θ range of 14–30°. A summary of the fundamental crystal data is given in Table 1, and the final values of all refined atomic coordinates are given in Table 2.

The complex crystallized in the $C2/c$ space group with only half independent crystallographic molecule, containing a 2-fold axis which passes through the middle of a hypothetical line between the rhodium atoms.

Three standard reflections were monitored after every 97 reflections and no appreciable decay in their intensities was observed. The structure was solved by Patterson and Fourier methods and refined by full-matrix least-squares on F^2 [24].

All non-hydrogen atoms were refined anisotropically. The hydrogen atoms were calculated, except that bonded to C10 which was located as the first peak in a difference Fourier synthesis, and then included and their positions fixed. The largest residual peak in the final difference map was 0.447 e \AA^{-3} in the vicinity of the rhodium atom. Most of the calculations were carried out with SHELX-97.

3. Results and discussion

3.1. Synthetic studies

Reaction of the chloro-dimers $[\text{Rh}(\mu\text{-Cl})(\text{L}_2)]_2$ ($\text{L}_2 = \text{COD}$, NBD) with a stoichiometric ratio of Hpz^{Fc} under nitrogen at r.t. and using MeOH/KOH or $\text{CH}_2\text{Cl}_2/\text{NEt}_3$ as proton abstractor media gave rise to the complexes $[\text{Rh}(\mu\text{-pz}^{\text{Fc}})(\text{L}_2)]_2$ ($\text{L}_2 = \text{NBD}$ (**1**), COD (**2**)) (Scheme 1). On treatment with carbon monoxide diolefin ligands were displaced from either one to give the tetracarbonyl dimer $[\text{Rh}(\mu\text{-pz}^{\text{Fc}})(\text{CO})_2]_2$ (**3**) (Scheme 1).

The complexes **1** and **2** were orange and yellow–orange solids, respectively, slightly air and moisture sensitive. The carbonyl derivative **3** was a stable yellow–orange solid. All complexes were characterized by analytical and spectroscopic IR and NMR (¹H- and ¹³C-) methods and mass spectrometry. Structure determination by X-ray diffraction of compound **2** was also achieved. Tables 3, 7 and 8 show the NMR, electronic and electrochemical data of the new complexes, respectively.

Table 1
Crystal and refinement data for **2**

Empirical formula	$\text{C}_{42}\text{H}_{46}\text{Fe}_2\text{N}_4\text{Rh}_2$
Formula weight	924.35
Crystal system	Monoclinic
Space group	$C2/c$
a (Å)	19.848(2)
b (Å)	12.274(1)
c (Å)	14.951(4)
β (°)	93.91(2)
V (Å ³)	3634(1)
Z	4
$F(000)$	1872
ρ_{calc} (g cm ⁻³)	1.690
Temperature (K)	293
μ (mm ⁻¹)	1.712
Crystal dimensions (mm)	0.17 × 0.17 × 0.10
Diffractometer	Enraf–Nonius CAD4
Radiation	Graphite-monochromated Mo–K α ($\lambda = 0.71073$ Å)
Scan technique	$\omega/2\theta$
Data collected	(–23, 0, 0) to (23, 14, 17)
θ range (°)	1.95–24.96
Independent reflections	3059 [$R_{\text{int}} = 0.0181$]
Data/restraints/parameters	3059/0/226
Total R indices [$I > 2\sigma(I)$] ^a	0.0276 (2349 reflections)
wR (all data) ^b	0.0834
Goodness-of-fit on F^2	0.824
Largest difference peak and hole (e \AA^{-3})	0.447 and –0.591

^a $\Sigma[|F_o| - |F_c|]/\Sigma|F_o|$.

^b $(\Sigma[w(F_o^2 - F_c^2)^2]/\Sigma[w(F_o^2)^2])^{1/2}$.

Table 2

Atomic coordinates ($\times 10^4$) and equivalent isotropic displacement parameters ($\text{\AA}^2 \times 10^3$) for **2**

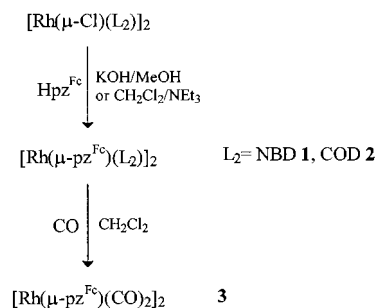
Atom	x	y	z	U_{eq}^a
Rh(1)	4504(1)	7670(1)	1615(1)	34(1)
Fe(2)	3171(1)	11350(1)	1528(1)	41(1)
N(1)	4631(2)	8589(3)	3442(3)	39(1)
N(2)	4257(2)	8715(3)	2650(2)	34(1)
C(3)	3776(2)	9474(3)	2762(3)	39(1)
C(4)	3842(3)	9821(4)	3652(3)	54(1)
C(5)	4372(3)	9252(4)	4042(3)	49(1)
C(6)	3298(2)	9806(3)	2034(3)	39(1)
C(7)	2626(2)	10192(4)	2136(4)	50(1)
C(8)	2326(3)	10437(4)	1261(4)	54(1)
C(9)	2806(3)	10209(4)	627(4)	52(1)
C(10)	3401(3)	9835(4)	1099(3)	46(1)
C(11)	3840(3)	12330(4)	2225(5)	62(2)
C(12)	3194(3)	12711(4)	2318(4)	61(2)
C(13)	2889(4)	12946(4)	1482(5)	79(2)
C(14)	3352(5)	12736(5)	846(5)	98(3)
C(15)	3952(4)	12338(5)	1308(6)	86(2)
C(16)	3493(3)	7091(5)	1425(5)	69(2)
C(17)	3854(3)	6430(4)	2033(5)	62(2)
C(18)	4103(3)	5309(5)	1833(6)	89(2)
C(19)	4580(4)	5267(5)	1130(5)	91(2)
C(20)	4889(3)	6358(5)	877(4)	65(2)
C(21)	4554(4)	7088(5)	289(4)	69(2)
C(22)	3862(5)	6913(8)	-153(5)	120(3)
C(23)	3322(4)	6763(8)	480(7)	125(4)

^a U_{eq} is defined as one third of the trace of the orthogonalized U_{ij} tensor.

3.2. Spectroscopic studies

The IR spectra of complexes **1** and **2** in KBr pellets showed the characteristic bands from the diolefin ligands and pyrazolato rings [17,19]. Absorption bands at ca. 1105 and 810 cm^{-1} were assigned to the $\nu(\text{CC})$ and $\pi(\text{CH})$ vibrations of the cyclopentadienyl rings of the ferrocenyl substituent [25]. Complex **3** exhibited three carbonyl bands both in the solid state and in dichloromethane solution, one broad and two sharp, in agreement with the pattern observed in related dimeric tetracarbonyl species [17,19].

Complexes **1–3** showed intense molecular-ion peaks in FAB⁺ mass spectrometry with their corresponding



Scheme 1.

isotopic patterns as well as varying number of fragments. In all spectra fragments due to the sequential loss of ligands were observed. We also found peaks of low intensity corresponding to the loss of a cyclopentadienyl moiety.

As it has been described in previous works [17,19,26], owing to the unsymmetrical substitution of bridging pyrazolate ligands the dinuclear complexes $[\text{Rh}(\mu\text{-pz}^{\text{Fc}})(\text{L}_2)_2]$ can exist as two geometrical isomers, containing the two pyrazolate bridges oriented head-to-head (H-H) having a C_s symmetry and head-to-tail (H-T) having a C_2 symmetry, as depicted in Fig. 1.

The ¹H- and ¹³C-NMR spectra of **1** and **2** were compatible with the presence of only one isomer having two equivalent diolefin ligands, i.e. the H-T isomer (Table 3).

For **1** the ¹H-NMR spectrum gave rise to eight signals at r.t. due to the diolefin moiety, consistent with the inequivalent eight protons of the NBD ligands. This proposal was also confirmed by using homonuclear (¹H-¹H)COSY experiment. Hence, all NBD signals could be themselves related, in agreement with the equivalence of the two NBD ligands in a H-T isomer. The methylene protons at 1.42 and 1.12 ppm were coupled with the tertiary proton at 4.15 ppm, but the coupling with the other tertiary proton was not observed. The olefinic protons at 3.98 and 3.52 ppm were coupled with the tertiary proton at 4.15 ppm. The remaining olefinic and tertiary protons were then assigned to the resonances at 4.29, 3.79 and 4.10 ppm, respectively from their corresponding couplings.

The ¹H-NMR spectrum of **2** was more complex than that of **1** in relation to the diolefin moiety. Four broad CH-olefinic signals at 4.59, 4.13, 4.06 and 3.66 ppm and six CH₂-ethylene signals as multiplets in the range 2.9–1.6 ppm were observed (Table 3). In principle, because four CH-olefinic signals were expected both in the H-H and in the H-T isomers, the above results were not conclusive to establish the isomer produced. However taking into account that the H-T configuration appears to be favoured by bulky substituents and ancillary ligands [16,17,19], that isomeric form could be suggested for **2**. As for **1** the assignment of the resonances was performed using homonuclear (¹H-¹H)COSY experiment, from which an equivalence of the COD ligands was deduced through the relation established between all olefinic and aliphatic protons. The olefinic protons appeared as four signals showing couplings between those at 4.59 and 4.13 ppm and 4.06 and 3.66 ppm, respectively. The *exo* and *endo* CH₂-protons ranged from 2.90 to 2.15 and 2.10 to 1.55 ppm as three 1:2:1 and 2:1:1 signals in each group, respectively.

The most important feature consistent with the H-T isomer in both cases was related to the presence of only one type of pyrazolate group deduced from the signals corresponding to the H4 and H5 protons at 6.13 and

Table 3
NMR data of compounds **1–3**

	pz	Fc ^a	L ₂
¹ H-NMR			
1	H4: 6.13d H5: 7.16d <i>J</i> ₄₅ = 1.8	C ₅ H ₅ : 4.04 C ₅ H ₄ : 4.30, 4.46, 4.52, 5.98	CH-1,4: 4.10, 4.15 CH-2,3,5,6: 3.52, 3.79, 3.98, 4.29 CH ₂ -7: 1.12, 1.42
2	H4: 6.17d H5: 7.42d <i>J</i> ₄₅ = 1.8	C ₅ H ₅ : 3.77 C ₅ H ₄ : 4.21, 4.32, 4.40, 6.47	CH-1,2,5,6: 3.66, 4.06, 4.13, 4.59 CH ₂ -3,4,7,8: 1.6–2.9
3a ^b	H4: 6.42d H5: 7.52d <i>J</i> ₄₅ = 1.8	C ₅ H ₅ : 4.07 C ₅ H ₄ : 4.35, 4.39, 4.79, 5.26	
3b ^b	H4: 6.38d H5: 7.56d <i>J</i> ₄₅ = 1.8	C ₅ H ₅ : 3.95 C ₅ H ₄ : 4.29, 4.35, 4.62, 5.53	
¹³ C-NMR			
1	C3: 148.5 C4: 103.8 C5: 137.6	C ₅ H ₅ : 69.4 C ₅ H ₄ : 67.5, 67.6, 67.8, 80.2	CH-1,4: 50.9, 51.3 CH-2,3,5,6: 57.1, 58.5 CH ₂ -7: 61.8
2	C3: 150.5 C4: 102.7 C5: 137.2	C ₅ H ₅ : 69.5 C ₅ H ₄ : 67.2, 67.3, 67.6, 68.2, 79.7	CH-1,2,5,6: 77.1d, 81.3d, 81.6d, 82.5d <i>J</i> _{Rh} = 11–13 CH ₂ -3,4,7,8: 29.4, 30.9, 31.9, 32.0
3a ^b	C3: 151.6 C4: 104.8 C5: 142.6	C ₅ H ₅ : 69.5 C ₅ H ₄ : 68.1, 68.2, 68.5, 68.6, 78.4	CO: 184.3d <i>J</i> _{Rh} = 67 184.3d <i>J</i> _{Rh} = 76
3b ^b	C3: 151.9 C4: 104.5 C5: 141.4	C ₅ H ₅ : 69.4 C ₅ H ₄ : 67.6, 68.2, 68.3, 68.5, 78.1	CO: 185.4d <i>J</i> _{Rh} = 73 185.5d <i>J</i> _{Rh} = 70

^a Fc = (η⁵-C₅H₄)Fe(η⁵-C₅H₅).

^b **3a** and **3b** are the major and minor isomers, respectively.

7.16 ppm for **1** and 6.17 and 7.42 ppm for **2**, respectively. These signals were clearly resolved as doublets (³*J* = 1.8 Hz) at r.t. suggesting a static nature of the complexes.

On the other hand, five signals were observed for the ferrocenyl fragment, one corresponding to the C₅H₅ ring and four of the C₅H₄ ring. It was interesting to note that one of the resonances of the C₅H₄ protons of the ferrocenyl substituent was strongly shifted towards lower field than that frequently observed in other ferrocenyl derivatives [10–12,27]. The deshielding of this proton (5.98 and 6.47 ppm for **1** and **2**, respectively) could be explained by considering the presence of a weak interaction between this proton and the rhodium atom.

The ¹³C-NMR spectra of **1** and **2** (Table 3) showed the olefinic carbon resonances as well resolved doublets in agreement with the proposed static nature of the complexes.

As has already been mentioned, the ¹H-NMR signals of the NBD and COD ligands were slightly broad, this fact probably suggesting motions of the ligands. However, the well resolved olefinic carbon signals again indicated rigidity of these complexes on the NMR time-scale at r.t.

The crystalline structure of **2** was solved in order to structurally characterize the isomer formed. From that, as will be described below, the H-T configurational isomer exhibiting a Rh(NN)₂Rh metallocyclic core was evidenced.

Then the proposed Rh–H interaction between the rhodium atom and one of the C₅H₄ protons of the ferrocenyl substituent, albeit of a weak type, should favour a more rigid structure making contributions to the lack of the inversion of the Rh(NN)₂Rh boat [19,28,29].

The ¹H and ¹³C-NMR spectra of the carbonyl derivative **3** were in agreement with a mixture of both H-H and H-T isomers, **3a** and **3b** (Table 3). Two signals for each H4 and H5 protons of the pyrazolate rings were

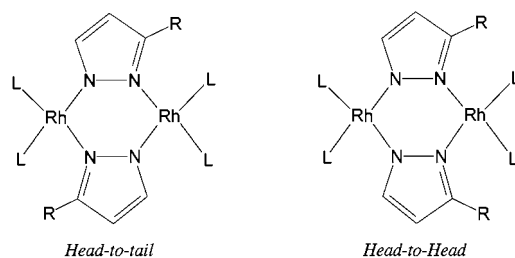


Fig. 1. H-H and H-T configurational isomers for [Rh(μ-pz^R)(L₂)₂]₂.

Table 4

Selected bond distances (Å) and angles (°) for **2** with estimated S.D. in parentheses ^{a,b,c}

Bond distance (Å)			
Rh1··Rh1A	3.189(1)	N1–N2	1.363(5)
Rh1–N2	2.093(3)	N2–C3	1.352(5)
Rh1–N1A	2.061(4)	C3–C4	1.395(7)
Rh1–C16	2.128(5)	C4–C5	1.362(7)
Rh1–C17	2.116(5)	N1–C5	1.339(6)
Rh1–C20	2.125(5)	C3–C6	1.453(6)
Rh1–C21	2.117(5)	Fe2–C610	1.640(5)
Rh1–C1617	2.005(5)	Fe2–C1115	1.648(7)
Rh1–C2021	2.003(6)	C10–H10	0.927
Rh1··H10	2.877		
Bond angles (°)			
N1A–Rh1–N2	86.2(1)	N1A–Rh1–C2021	93.5(2)
N2–Rh1–C2021	177.2(2)	N1A–Rh1–C1617	177.6(2)
N2–Rh1–C1617	92.6(2)	Rh1–H10–C10	125

^a C1617 and C2021 are the midpoints of (C16, C17) and (C20, C21), respectively.

^b C610 and C1115 are the midpoints of the substituted and unsubstituted cyclopentadienyl rings, respectively.

^c Symmetry code (A): $-x+1, y, -z+1/2$.

observed in the ¹H-NMR spectrum and the remaining signals of the ferrocenyl substituents were also duplicated. The ¹³C-NMR spectrum showed four doublets for the carbon atoms of the carbonyl groups bonded to the rhodium atoms, two from each isomer. A ratio of the isomers of 55/45 was determined by integration of the resonances of the H4 protons and the C4 signals of the pyrazolate ring. The homonuclear (¹H–¹H)COSY experiment confirmed the presence of the mixture of isomers showing the corresponding couplings.

The assignment of the proton resonances of **3** allowed us to observe a high deshielding of one of the protons of the C₅H₄ group of each isomer (5.53 and 5.26 ppm), consistent with the presence of Rh–H interactions as in the above cases. Then, by comparison of such a chemical shift at lower field of one of the C₅H₄ protons observed in complexes **1–3**, the Rh–H interaction appeared to be depending on the ancillary ligands and it should be ranged in the order COD > NBD > 2CO.

3.3. Crystal structure of $[Rh(\mu\text{-}pz^{Fc})(COD)]_2$ (**2**)

In order to establish the isomer formed and to obtain more information about potential intramolecular interactions in the solid state we solved the crystalline structure of $[Rh(\mu\text{-}pz^{Fc})(COD)]_2$ (**2**). Table 4 lists selected bond distances and angles and Table 5 shows selected angles between the least-squares sets defined by specified atoms [30].

The X-ray structure confirmed the dimeric nature of the compound formed by two rhodium atoms, two pyrazolate rings bridging the two metals and two di-

Table 5

Selected angles (°) between the least-squares sets defined by the specified atoms for **2** ^{a,b}

1. N1A, N2, C1617, C2021	1–2	74.6(1)
2. N1, N2A, C16A17A, C20A21A	1–5	52.6(2)
3. Rh1, N2, N1, Rh1A	1–6	89.5(2)
4. Rh1, N1A, N2A, Rh1A	1–7	71.0(1)
5. N1, N2, N1A, N2A	3–4	81.1(1)
6. C16, C17, C20, C21	7–8	87.4(2)
7. N1, N2, C3, C4, C5	7–9	29.5(2)
8. N1A, N2A, C3A, C4A, C5A		
9. C6, C7, C8, C9, C10		

^a C1617 and C2021 are the midpoints of (C16, C17) and (C20, C21), respectively.

^b Symmetry code (A): $-x+1, y, -z+1/2$.

olefinic ligands. The structure was built around a central nonplanar cyclic core which closely resembled that encountered in analogues complexes described previously [15–20,31,32]. That is, each rhodium atom exhibited a square-planar coordination, and the two rhodium and the four nitrogen atoms of the two bridged pyrazolato ligands gave rise to a metallocycle Rh(NN)₂Rh ring in a boat conformation. Fig. 2 shows an ORTEP perspective and it emphasizes the way in which close approach of the two rhodium atoms was made possible by the bending of the bridging into a characteristic boat-shaped conformation. The substituents on the pyrazolate rings opposed each other along the intermetallic axis, i.e. adopted a relative position corresponding to the H-T configuration in keeping with the spectroscopic results.

In this arrangement the rhodium atoms approached each other to within 3.189(1) Å, corresponding to the inclination between the two independent coordination planes about rhodium of 74.6(1)° as well as to the

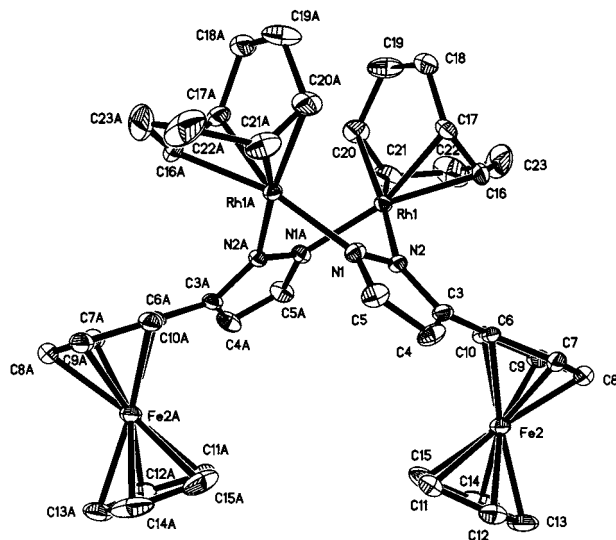


Fig. 2. Perspective ORTEP of **2**. The hydrogen atoms have been omitted for clarity.

Table 6
Structural parameters for complexes $[\text{Rh}(\mu\text{-pz}^{\text{R}})(\text{COD})]_2$

Compound	Rh...Rh (Å)	α^a (°)	β^a (°)	Ref.
$[\text{Rh}(\mu\text{-pz}^{\text{Me}_2})(\text{COD})]_2$	3.154	71.7		[15]
$[\text{Rh}(\mu\text{-pz}^{\text{Fc}})(\text{COD})]_2$	3.189	74.6	81.1	This work
$[\text{Rh}(\mu\text{-pz}^{\text{PhOPh}})(\text{COD})]_2$	3.219	77.1	100.1	[19]
$[\text{Rh}(\mu\text{-pz}^{\text{PhOBu}})(\text{COD})]_2$	3.234	78.5	101.7	[19]
$[\text{Rh}(\mu\text{-pz})(\text{COD})]_2$	3.267	80.7		[33]

^a α is the dihedral angle between the coordination planes of the two rhodium metals and β is the dihedral angle between the two RhN-NRh planes [18].

dihedral angles between the two Rh–N–N–Rh planes of 81.1(1)° and between the plane defined by the four nitrogen atoms and the N–Rh–N plane of 52.7(2)°.

For comparative purposes some of these parameters from complexes $[\text{Rh}(\mu\text{-pz}^{\text{R}})(\text{COD})]_2$ are listed in Table 6. The relative folding of these structures was clearly depending on the substituents on the pyrazol rings and associated with the metal–metal distance.

It was also clear that the short but formally non-bonding Rh...Rh distance may reflect some degree of metal–metal interaction [17–19].

The orthogonal orientation of the COD ligands was deduced from the value of the dihedral angle between the plane formed by the four olefinic carbon atoms and the coordination plane of 89.5(2)°.

The bridged pyrazolato ligands were situated in a position between normal and parallel as deduced by the dihedral angles between the coordination and the pyrazolato planes of 71.0(1)°.

The COD ethylenic hydrogen atoms attached to the C18–C19A pair were located at a nonbonding distance of 2.37 Å, which was very short in relation to the Van der Waals radius for hydrogen. Then, a significantly closer approach between the corresponding carbon atoms of the opposing COD ligand was evidenced, suggesting structurally significant nonbonding interaction [15,16,34].

The orientation of the C_5H_4 group of the ferrocenyl substituent on the pyrazol ring merits further comments. The cyclopentadienyl C_5H_5 and C_5H_4 rings of the ferrocenyl substituent were parallel (0.4(2)°) and they adopted a staggered conformation. The dihedral angle between the C_5H_4 and pyrazole planes of 29.5(2)°, slightly lower than that observed in related complexes containing aryl substituent [19], indicated an adequate orientation of the C_5H_4 group to give rise to a proximity of the rhodium center and the H10 of the C_5H_4 ring, yielding a Rh–H10 distance of 2.877 Å. Although this distance was longer than separations of the agostic type, which range from 1.8 to 2.2 Å [29], it was shorter than the sum of the van der Waals radii suggesting a weak interaction in the solid state, which could be

considered as of preagostic type [19,35]. This proposal was also consistent with the interaction suggested from the solution studies.

3.4. Electronic studies

The electronic spectra of the complexes **1–3** were recovered in dichloromethane solution. For comparative purposes the spectrum of the 3(5)-(ferrocen-1-yl)pyrazole ligand was also considered [11]. The main absorption data are listed in Table 7.

The spectrum of Hpz^{Fc} exhibited two spin-allowed d–d absorptions from the ferrocene centered at 326 and 443 nm [11,36] and another absorption at a higher energy (273 nm) attributed to a metal–ligand charge-transfer transition [11]. The shoulder at 219 nm was assigned to $\pi\text{-}\pi^*$ pyrazole transition [11,37]. By comparing these data with those for ferrocene [25] it could be considered that pyrazolyl substitution on the ferrocene has no significant effect on the energies of the d–d transitions.

The spectra of **1–3** showed in the visible region two absorption bands in the range of 340–400 and 395–490 nm, respectively. For complexes **1** and **2** an additional band in the ultraviolet region centered at 280 nm was observed. All bands had high absorption coefficients which provided evidence of charge-transfer transitions.

The lowest-energy absorptions in **1** and **2** could be considered ferrocenyl d–d transition bands, superposed probably with rhodium–ligand and iron–ligand ($d\text{-}\pi^*$) charge-transfer bands [12]. These transitions showed bathochromic shifts related to those of the ligand itself. In addition the red shift of the lowest-energy band was higher in **1** than in **2**, reflecting the electron withdrawing character of the ancillary ligands.

For **3** the absorption band at 340 nm was consistent with a metal–ligand charge-transfer transition in which the CO ligands should be implicated [38]. The other band at 400 nm was assigned to superposed metal–ligand charge-transfer and ferrocenyl d–d transitions as in the above diolefinic compounds.

The highest-energy band at 280 nm observed in **1** and **2** was absent in **3**, and it was consistent with charge-

Table 7
UV–vis spectroscopic data for compounds Hpz^{Fc} and **1–3**

Compound	λ_{max} (nm) (ϵ dm ³ mol ⁻¹ cm ⁻¹) ^a
Hpz^{Fc}	219 (sh), 273 (9100), 326 (sh), 443 (230) ^b
1	282 (21750), 388 (2700), 487 (3500)
2	281 (20000), 360 (3000), 452 (3900)
3	345 (6000), 395 (4000)

^a All spectra were registered in dichloromethane solutions with concentrations of ca. 10^{-4} M.

^b Ref. [11].

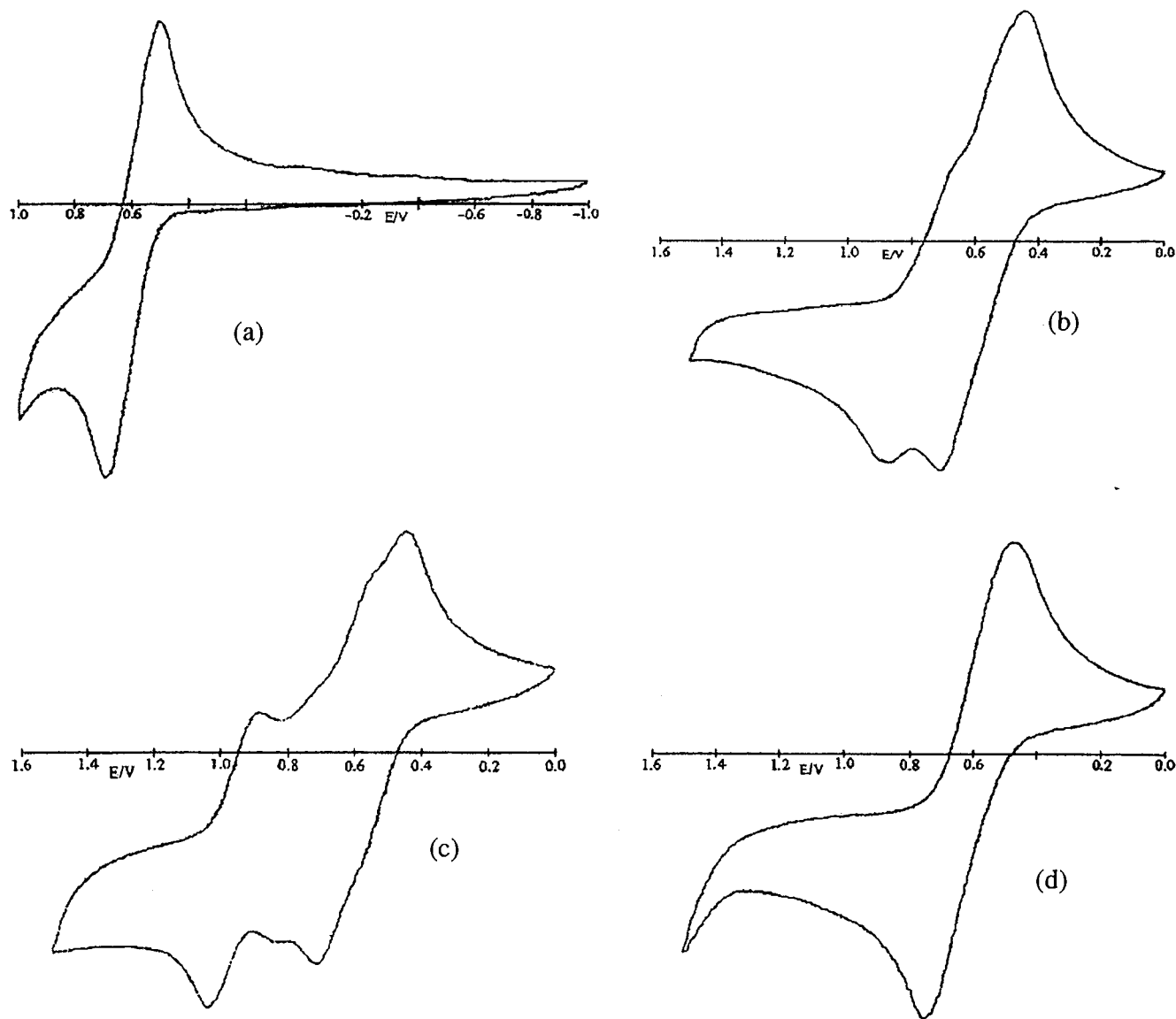


Fig. 3. Voltammograms of (a) Hpz^{Fc} ; (b) complex **1**; (c) complex **2** and (d) complex **3** in dichloromethane.

transfer transition in which the diolefin ligands should be implicated.

3.5. Electrochemical studies

The electrochemical behavior of **1–3** was investigated by cyclic voltammetry in dichloromethane solution. The data of the 3(5)-(ferrocen-1-yl)pyrazole ligand was also included in this study for comparative purposes [11]. Fig. 3 shows the voltammograms for each complex and Hpz^{Fc} ligand, and Table 8 shows the electrochemical data.

In all cases a quasireversible wave at ca. 0.59 V was observed and assigned to $\text{Fe}^{\text{II}}/\text{Fe}^{\text{III}}$ oxidation of the ferrocenyl moiety by comparison of these potentials with those of ferrocene itself and other complexes with ferrocenylpyridine [10].

The diolefinic derivatives **1** and **2** showed one or two additional oxidation waves at E_p^{a} of 0.90 V for **1** and 0.81 and 1.04 V for **2** with associated daughter reduction peaks. These oxidation waves were assigned to the rhodium(I) centers and compared with those obtained

Table 8
Electrochemical data for compounds Hpz^{Fc} and **1–3**

Compound	E_f ($\text{Fe}^{\text{II}}/\text{Fe}^{\text{III}}$) (V)	Other peaks	
		E_p^{a} (V)	E_p^{c} (V)
Hpz^{Fc}	0.59		
1	0.59	0.90	0.66
2	0.58	0.81, 1.04	0.91, 0.56
3	0.61		
4		0.66, 1.60	1.01, 0.42

for the related complex $[\text{Rh}(\mu\text{-pz}^{\text{Bu}})(\text{NBD})_2]$ (**4**) [17] containing pyrazolato ligands without ferrocenyl substituents. The latter exhibited two oxidation waves at E_p^{a} of 0.66 and 1.60 V and two reduction waves at E_p^{c} of 1.01 and 0.42 V.

Similar electrochemical results have been described for the binuclear rhodium(I) complexes $[\text{Rh}_2(\text{CO})_4(\text{Dcbp})]^-$ (Dcbp = trianion of 3,5-pyrazoledicarboxylic acid) [39] and $[\text{Rh}_2(\text{CO})_4(\text{Mdcbi})]^-$ (Mdcbi = trianion of 2-methylimidazole-4,5-dicarboxylic acid) [40] for which a complete electrochemical study was carried out [40]. On these basis the oxidation processes $\text{Rh(I)}-\text{Rh(I)} \rightarrow \text{Rh(I)}-\text{Rh(II)} \rightarrow \text{Rh(II)}-\text{Rh(II)}$ were suggested to explain the oxidation waves observed for complexes **1**, **2** and **4**.

The irreversible reduction peaks in complexes **1**, **2** and **4** were tentatively assigned to Rh-based reductive processes.

By comparing complexes **1** and **4** having the same ancillary NBD ligand the oxidation processes were cathodically shifted from non-ferrocenyl complex **4** to the ferrocenyl derivative **1** according with the presence of the substituent on the pyrazole ring. Then it was possible to suggest that in **1** the more cathodic oxidation process on the rhodium atoms could be occluded by the ferrocenyl oxidation. The same feature could be responsible for the single oxidation peak observed in **3**.

Upon reduction no waves were observed when potentials were scanned to -2 V.

When complexed in **1–3** the ferrocene oxidation waves of the ferrocenylpyrazolato ligand were almost unchanged indicating that the rhodium(I) center did not affect the electron density on the ferrocenyl moiety similar to that found for ferrocenylbipyridine and ferrocenylpyridine derivatives [41]. However, for the $\text{Fe}^{\text{II}}/\text{Fe}^{\text{III}}$ oxidation previous works on ferrocenylpyrazole derivatives suggested that inductive effects were not the only factors influencing on the oxidation potential values if conjugation effects should also be considered [10,42].

In our complexes the substituent on ferrocenyl was an aromatic planar ring (pyrazolate) which may be conjugated with the cyclopentadienyl ring. This effect should decrease the oxidation potential of the ferrocenyl group as has been proved on 3-ferrocenylpyrrole [42]. In turn effects produced by complexation associated with the electrodonating nature of the pyrazolato ligands could produce the opposite effect and compensate such shifts. So, in complexes **1–3** the oxidation potential on the ferrocenyl moiety was almost unmodified with respect to the free ligand (Table 8).

4. Conclusions

In summary, the new dimeric $[\text{Rh}(\mu\text{-pz}^{\text{Fc}})(\text{L}_2)]_2$ ($\text{L}_2 = \text{NBD}, \text{COD}, 2\text{CO}$) complexes (**1–3**) with a ferrocenyl

substituent on the pyrazole ring have been shown to have the H-T configuration when bulky ancillary ligands (NBD, COD) were present, but the H-H isomer was also formed for the less-demanding CO ligands. The solution studies evidenced the existence of Rh–H interactions which appeared to make contributions to the lack of dynamic behavior.

The X-ray diffraction studies on $[\text{Rh}(\mu\text{-pz}^{\text{Fc}})(\text{COD})]_2$ confirmed the identity of the H-T isomer with Rh...Rh distance related to the structural folding of the boat-shaped $\text{Rh}(\text{NN})_2\text{Rh}$ ring produced by the ferrocenyl substituent.

These new complexes showed metal–ligand charge-transfer transitions and maintained an almost unchanged oxidation potential in the ferrocenyl group.

All these results suggest that the complexes could be adequate as building blocks in the design of molecules with nonlinear optical properties.

5. Supplementary material

Tables giving fractional coordinates and thermal parameter, bond distances and angles, and observed and calculated structure factors for **2** (3, 8 and 11 pages, respectively) are available from the author on request.

Acknowledgements

We thank the DGES of Spain for financial support (project PB95-0370).

References

- [1] (a) E. Amouyal, M. Mouallem-Bahout, *J. Chem. Soc. Dalton Trans.* (1992) 509. (b) V. Balzani, F. Scandola, *Supramolecular Chemistry*, Horwood, Chichester, 1991.
- [2] (a) C.K. Ryu, R. Wang, R.H. Schmehl, S. Ferrere, M. Ludwikow, J.W. Merkert, C.E.L. Headford, C.M. Elliot, *J. Am. Chem. Soc.* 114 (1992) 430. (b) V. Balzani, L. De Cola, *Supramolecular Chemistry*, Kluwer, Dordrecht, 1992. (c) D. Gust, T.A. Moore, A.L. Moore, *Acc. Chem. Res.* 26 (1993) 198.
- [3] (a) J.C. Calabrese, L.T. Cheng, J.C. Green, S.R. Marder, W. Tam, *J. Am. Chem. Soc.* 113 (1991) 7227. (b) A. Houlton, N. Jasim, R.M.G. Roberts, J. Silver, D. Cunningham, P. McArdle, T. Higgings, *J. Chem. Soc. Dalton Trans.* (1992) 2235. (c) N.J. Long, *Angew. Chem. Int. Ed. Engl.* 34 (1995) 21.
- [4] (a) P.D. Beer, *Chem. Soc. Rev.* 18 (1989) 409. (b) J.C. Medina, I. Gay, Z. Chen, L. Echegoyen, G.W. Gokel, *J. Am. Chem. Soc.* 113 (1991) 365. (c) M.D. Ward, *Chem. Soc. Rev.* 24 (1995) 121.
- [5] (a) M. Sawamura, Y. Ito, *Chem. Rev.* 92 (1992) 857. (b) H.B. Kagan, P. Diter, A. Gref, D. Guillauneux, A. Masson-Szymczak, F. Rebiere, O. Riant, O. Samuel, S. Taudien, *Pure Appl. Chem.* 68 (1996) 29.
- [6] (a) P.D. Beer, O. Kocian, R.J. Mortimer, P. Spencer, *J. Chem. Soc. Chem. Commun.* (1992) 602. (b) P.D. Beer, J.E. Nation, M.E. Harman, M.B. Hursthouse, *J. Organomet. Chem.* 441 (1992) 465. (c) G. De Santis, L. Fabbrizzi, M. Licchelli, C.

- Mangano, P. Pallavicini, A. Poggi, *Inorg. Chem.* 32 (1993) 854.
- (d) C. Dongli, J. Handong, Z. Hongyun, C. Deji, Y. Jina, L.B. Jian, *Polyhedron* 13 (1994) 57.
- [7] (a) K. Schlögl, A. Mohar, *Monatsh. Chem.* 93 (1962) 861. (b) K. Schlögl, H. Egger, *Monatsh. Chem.* 94 (1963) 1054.
- [8] (a) S. Trofimenko, *Prog. Inorg. Chem.* 34 (1986) 115. (b) P.K. Byers, A.J. Canty, R.T. Honeyman, *Adv. Organomet. Chem.* 34 (1992) 1. (c) S. Trofimenko, *Chem. Rev.* 93 (1993) 943. (d) N. Kitajima, W.B. Tolman, *Prog. Inorg. Chem.* 43 (1995) 419. (e) G. Parkin, *Adv. Inorg. Chem.* 42 (1995) 291.
- [9] K. Niedenzu, J. Serwatowski, S. Trofimenko, *Inorg. Chem.* 30 (1991) 524.
- [10] N. Chabert, L. Jacquet, C. Marzin, G. Tarrago, *New J. Chem.* 19 (1995) 443.
- [11] R.J. Lees, J.L.M. Wicks, N.P. Chatterton, M.J. Dewey, N.L. Cromhout, M.A. Halcrow, J.E. Davies, *J. Chem. Soc. Dalton Trans.* (1996) 4055.
- [12] N. Chabert-Couchouren, C. Marzin, G. Tarrago, *New J. Chem.* 21 (1997) 355.
- [13] C. López, R.M. Claramunt, S. Trofimenko, J. Elguero, *Can. J. Chem.* 71 (1993) 678.
- [14] A. Schnyder, A. Togni, U. Wiesli, *Organometallics* 16 (1997) 255.
- [15] K.A. Beveridge, G.W. Bushnell, S.R. Stobart, J.L. Atwood, M.J. Zaworotko, *Organometallics* 2 (1983) 1447.
- [16] G.W. Bushnell, D.O. Kimberley Fjeldsted, S.R. Stobart, M.J. Zaworotko, S.A.R. Knox, K.A. Macpherson, *Organometallics* 4 (1985) 1107.
- [17] C. López, J.A. Jiménez, R.M. Claramunt, M. Cano, J.V. Heras, J.A. Campo, E. Pinilla, A. Monge, *J. Organomet. Chem.* 511 (1996) 115.
- [18] C. Tejel, J.M. Villoro, M.A. Ciriano, J.A. López, E. Eguizábal, F.J. Lahoz, V.I. Bakhmutov, L.A. Oro, *Organometallics* 15 (1996) 2967 and references cited therein.
- [19] M. Cano, J.V. Heras, M. Maeso, M. Alvaro, R. Fernández, E. Pinilla, J.A. Campo, A. Monge, *J. Organomet. Chem.* 534 (1997) 159 and references cited therein.
- [20] L.A. Oro, M.A. Ciriano, C. Tejel, *Pure Appl. Chem.* 70 (1998) 779.
- [21] (a) J. Elguero, M. Esteban, M.F. Grenier-Loustalot, L.A. Oro, M.T. Pinillos, *J. Chim. Phys.* 81 (1984) 251. (b) J.A. Balley, S.L. Grundy, S.R. Stobart, *Organometallics* 9 (1990) 536. (c) M.A. Ciriano, M.A. Tena, L.A. Oro, *J. Chem. Soc. Dalton Trans.* (1992) 2123. (d) C. Tejel, M.A. Ciriano, L.A. Oro, A. Tiripicchio, M. Tiripicchio-Camellini, *Organometallics* 13 (1994) 4153, and references cited therein.
- [22] (a) E.W. Abel, M.A. Bennett, G. Wilkinson, *J. Chem. Soc.* (1959) 3178. (b) J. Chatt, L.M. Venanzi, *J. Chem. Soc.* (1957) 4735.
- [23] M. Cano, J.A. Campo, J.V. Heras, M.C. Lagunas, M. Ruiz-Bermejo, unpublished results
- [24] G.M. Sheldrick, SHELXL93, Program for Refinement of Crystal Structure, University of Göttingen, Germany, 1993.
- [25] M. Roseblum, *Chemistry of the Iron Group Metallocenes*, Wiley, New York, 1965.
- [26] F. Bonati, L.A. Oro, M.T. Pinillos, C. Tejel, B. Bovio, J. Organomet. Chem. 465 (1994) 267.
- [27] (a) C. López-Garabito, J.A. Campo, J.V. Heras, M. Cano, G. Rojo, F. Agulló, *J. Phys. Chem. B* 102 (1998) 10698. (b) B.J. Coe, C.J. Jones, J.A. McCleverty, D. Bloor, G.H. Cross, J. Organomet. Chem. 464 (1994) 225. (c) B.J. Coe, T.A. Hamor, C.J. Jones, J.A. McCleverty, D. Bloor, G.H. Cross, T.L. Axon, *J. Chem. Soc. Dalton Trans.* (1995) 673. (d) B.J. Coe, C.J. Jones, J.A. McCleverty, D. Bloor, P.V. Kolinsky, R.J. Jones, *Polyhedron* 13 (1994) 2107. (e) B.J. Coe, J.D. Foulon, T.A. Hamor, C.J. Jones, J.A. McCleverty, D. Bloor, G.H. Cross, T.L. Axon, *J. Chem. Soc. Dalton Trans.* (1994) 3425.
- [28] M.A. Ciriano, M.A. Tena, L.A. Oro, *J. Chem. Soc. Dalton Trans.* (1992) 2123.
- [29] M. Bortolin, U.E. Bucher, H. Rügger, L.M. Venanzi, A. Albinati, F. Lianza, S. Trofimenko, *Organometallics* 11 (1992) 2514.
- [30] M. Nardelli, *J. Appl. Crystallogr.* 28 (1995) 659.
- [31] (a) J.L. Atwood, K.A. Beveridge, G.W. Bushnell, K.R. Dixon, D.T. Eadie, S.R. Stobart, M.J. Zaworotko, *Inorg. Chem.* 23 (1984) 4050. (b) A.W. Coleman, D.T. Eadie, S.R. Stobart, M.J. Zaworotko, J.L. Atwood, *J. Am. Chem. Soc.* 104 (1982) 922.
- [32] G. La Monica, G.A. Ardizzoia, *Prog. Inorg. Chem.* 46 (1997) 151.
- [33] B.M. Louie, S.J. Rettig, A. Storr, J. Trotter, *Can. J. Chem.* 62 (1984) 1057.
- [34] J.L. Marshall, S.R. Stobart, H.B. Gray, *J. Am. Chem. Soc.* 106 (1984) 3027.
- [35] (a) A. Albinati, P.S. Pregosin, F. Wombacher, *Inorg. Chem.* 29 (1990) 1812. (b) C.G. Anklin, P.S. Pregosin, *Magn. Reson. Chem.* 23 (1985) 671. (c) A. Albinati, C.G. Anklin, F. Ganazzoli, H. Rügger, P.S. Pregosin, *Inorg. Chem.* 26 (1987) 503. (d) A. Albinati, C. Arz, P.S. Pregosin, *Inorg. Chem.* 26 (1987) 508.
- [36] (a) Y.S. Sohn, D.N. Hendrickson, H.B. Gray, *J. Am. Chem. Soc.* 93 (1971) 3603. (b) D.R. Kanis, M.A. Ratner, T.J. Marks, *J. Am. Chem. Soc.* 114 (1992) 10338.
- [37] J. Elguero, R. Jacquier, H.C.N.T. Duc, *Bull. Soc. Chim. Fr.* (1966) 3744.
- [38] G.L. Geoffroy, *Organometallic Photochemistry*, Academic Press, New York, 1979.
- [39] J.C. Bayón, G. Net, P. Esteban, P.G. Rasmussen, D.F. Bergstrom, *Inorg. Chem.* 30 (1991) 4771.
- [40] J.E. Anderson, T.P. Gregory, G. Net, J.C. Bayón, *J. Chem. Soc. Dalton Trans.* (1992) 487.
- [41] (a) J.C. Chambron, C. Coudret, J.P. Sauvage, *New J. Chem.* 16 (1992) 361. (b) B. Farlow, T.A. Nile, J.L. Walsh, A.T. McPhail, *Polyhedron* 12 (1993) 2891. (c) A.C. Benniston, V. Gouille, A. Harriman, J.M. Lehn, B. Marczinke, *J. Phys. Chem.* 98 (1994) 7798. (d) E.C. Constable, R. Martinez-Manez, A.M.W. Cargill Thompson, J.V. Walker, *J. Chem. Soc. Dalton Trans.* (1994) 1585.
- [42] T.L. Rose, A.B. Kon, *Inorg. Chem.* 32 (1993) 781.